RAPID COMMUNICATIONS

PHYSICAL REVIEW B VOLUME 52, NUMBER 2 1 JULY 1995-II

Critical scaling of the transport behavior and the magnetic phase diagram of polycrystalline $YBa_2Cu_3O_7$

Shi Li, M. Fistul, J. Deak, P. Metcalf, and M. McElfresh
Physics Department, Purdue University, West Lafayette, Indiana 47907
(Received 21 April 1995)

A magnetic phase diagram for polycrystalline $YBa_2Cu_3O_7$ was constructed using a combination of results from bulk magnetic and magnetotransport measurements. Electric field as a function of current density $E(J)$ can be scaled, with the critical coefficients $\nu \approx 1$ and $z \approx 4$, to identify the temperature of a phase transition into a state characterized by zero linear resistance. The magnetic-field dependence H of the critical current density J_c can be explained based on the penetration of magnetic flux between, and into, the individual grains of the polycrystalline material. The H dependence of the magnetization suggests that the individual crystallites of the polycrystalline material have low defect densities (clean).

In recent years a much more complete understanding of the magnetic phase diagram of the high-temperature superconductors (HTS), $YBa_2Cu_3O_7$ single crystals in particular, has emerged.[1,2] The vortex-solid transition is now generally accepted to be a true thermodynamic phase transition to a zero linear-resistance state that sets the crucial limits on the field and temperature range in which supercurrents can persist.[3–5] This more complete understanding now makes it possible to seek an understanding of the far more complex, yet technologically very important, polycrystalline HTS materials which exhibit many of the features of granular superconductors in addition to the already-complex phase behavior of HTS materials. Here a magnetic phase diagram for polycrystalline $YBa_2Cu_3O_7$ (poly-YBCO) is constructed using the results of a combination of magnetic and magnetotransport measurements.

Nearly randomly-oriented poly-YBCO was synthesized using standard ceramic preparation methods.[6] The average grain size and density was selected using special temperature-time profiles in environments for which the oxygen partial pressure was carefully controlled.[7] For these studies the material had a density of about 81% of theoretical and a median grain size of 8 μm. The superconducting transition temperature (T_c) was 91 K, and the transition width ΔT_c was about 2 K as measured by ac susceptibility at 2.5 MHz.

The field dependence of the bulk magnetization $M(H)$ was measured using a Quantum Design superconducting quantum interference device magnetometer after cooling in zero field. Measurements of the zero-field-cooled/field-cooled-cooling (ZFC/FCC) temperature-dependent magnetization, that are often used to determine the vortex-solid phase transition in single-crystal materials, were made as previously described.[8,9] Flux trapping was also studied using a method described previously.[10] A standard four-point probe technique[9] was used to measure electric field as a function of current density $E(J)$ at various fields and temperatures. A 1.7×10^{-8} V/cm E-field criteria was used to determine J_c from the $E(J)$ curves, however, only $E(J)$ curves with negative curvature were considered suitable for this determination.

Figure 1(a) shows $E(J)$ isotherms that range from $T=74$ K, starting from the lower right, to $T=90$ K in increments of 1 K for an 81%-dense sample of poly-YBCO in an applied field of 50 Oe. There is a single $E(J)$ isotherm (about 78 K) that exhibits power-law behavior $E\sim J^n$, with $n\approx 2.6$, over the full current-density range available. These $E(J)$ curves are quite similar to those of epitaxial YBCO thin films for which Ohmic behavior alone is observed at higher temperatures, then at intermediate temperatures curves with upward curvature that exhibit a crossing from Ohmic to power law are observed, and then curves with downward curvature alone are observed at temperatures below the transition to a state characterized by zero-linear resistance.[3] As shown in Fig. 1(b), the $E(J)$ data was analyzed using the scaling relation $E(J)\sim J\xi^{(1-z)}F_{\pm}(J\xi^2)$, where $\xi\sim|T-T_{cp}|^{-\nu}$ is a coherence length, ν and z are the spatial and dynamic critical exponents, respectively, and $F_{\pm}$ is a universal scaling function above (F_+) and below (F_-) the transition at T_{cp}.[1,3] For the results in Fig. 1(b), a transition temperature $T_{cp}=78.2$ K and critical scaling coefficients $\nu=0.9\pm0.1$ and $z=4.2\pm0.2$ were determined. This scaling behavior, and the coefficients observed, are nearly identical to those determined earlier ($\nu=1.1\pm0.2$ and $z=3.9\pm0.2$) for poly-YBCO.[11] The inset in Fig. 1 shows the transition temperature T_{cp} determined at various applied fields, $H_{cp}(T)$, using scaling over a range of fields. The values $\nu=1.0\pm0.1$ and $z=4.0\pm0.4$ were determined over the full range of fields studied. For $H_{cp}(T)$ two nearly-linear regions are observed with a large change in slope, from $dH_{cp}/dT=-7.4$ to -250 Oe/K, occurring when $T\approx 82$ K and $H\approx 50$ Oe.

The vortex-solid transition in single-crystal and epitaxial thin-film YBCO can be determined using the ZFC/FCC method.[8,9] The results of using this method with the 81%-dense sample of poly-YBCO are shown in Fig. 2. Clearly the ZFC/FCC-determined boundary lies at higher temperatures than $H_{cp}(T)$, suggesting that in poly-YBCO the vortex-solid transition is not the transition to a state characterized by zero-linear resistance. The ZFC/FCC boundary has a dependence given by $H_{ZFC/FCC}\sim(1-T/T_c)^x$, where $x\approx 2.5\pm0.7$. This compares with $x\approx 1.7$ observed for an epitaxial YBCO film for $H<10$ kOe. This dependence is more characteristic of the behavior observed for strongly-disordered single-

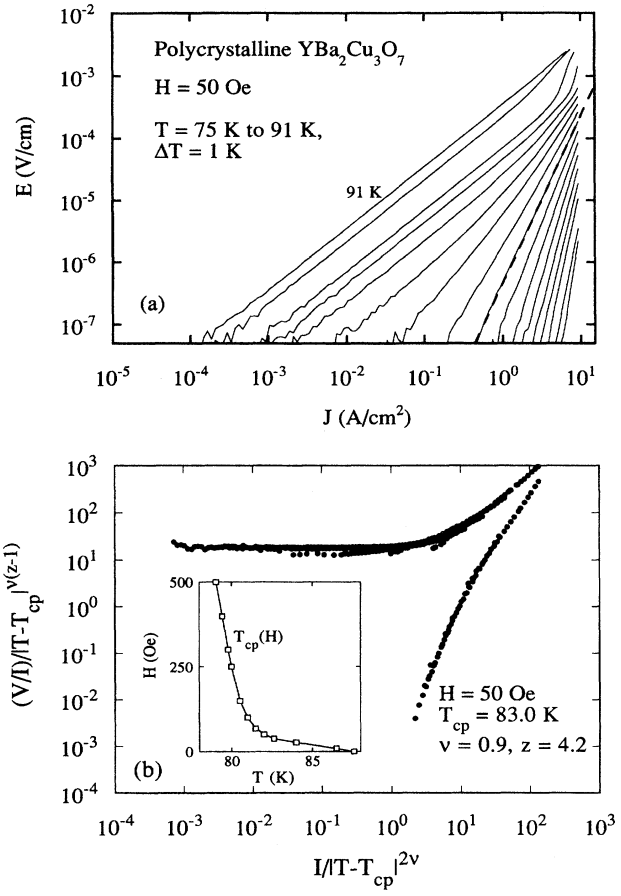

FIG. 1. (a) Electric field E as a function of current density J isotherms ranging from $T=74$ K at the lower right to $T=90$ K, in increments of 1 K for 81%-dense polycrystalline YBCO at $H=50$ Oe. (b) Critical scaling of the $E(J)$ data. A transition temperature $T_{cJ}=78.2$ K and critical scaling coefficients $\nu=0.9$ and $z=4.2$ were determined. The inset shows the field dependence of the transition temperature T_{cJ} determined by $E(J)$ scaling.

crystal and thin-film samples of YBCO than it is of the higher-temperature first-order–phase-transition boundary that characterizes very-clean YBCO single crystals.[12] The upper critical field H_{c2} determined using $M(T)$ measurements in YBCO single crystals is also plotted in Fig. 2.[13]

The magnetization as a function of applied field $M(H)$ for a bulk piece of 81%-dense poly-YBCO at $T=78$ K is shown in Fig. 3. A distinctive extremum, more evident in inset (a) of Fig. 3, is observed at $H_{pJ}\approx 7$ Oe. The field value of the peak at H_{pJ} and the initial slope of the $M(H)$ curve (below H_{pJ}) was studied as a function of the demagnetization field by selecting a set of samples of the same material having different geometries. The slope $dM/dH\approx -1/4\pi$ (cgs) was observed for the initial $M(H)$ curve for all the samples when the maximum-enclosed-ellipsoid demagnetization correction was applied. This result suggests that the bulk of the sample is screened up to the field H_{pJ}. Above H_{pJ} the $M(H)$ curve deviates from linearity, however, at a field H^*, not far above H_{pJ}, the slope again becomes linear. Starting at about H^* the slope is different than it is below H_{pJ} and $M(H)$ remains

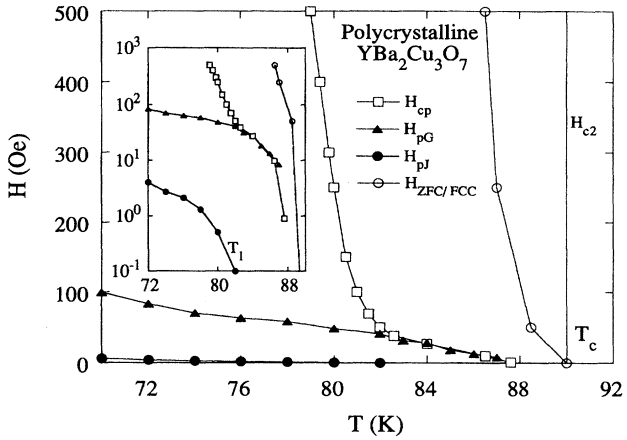

FIG. 2. Magnetic phase diagram incorporating the results of magnetotransport and bulk magnetic measurements. H_{cp} identifies the transition characterized by the onset of zero linear resistance and determined by scaling of $E(J)$ data, H_{pJ} is the field at which flux starts to penetrate into the bulk of the sample, H_{pG} is the field at which flux starts to penetrate into individual grains, $H_{ZFC/FCC}$ is the upper bound for irreversible behavior, and H_{c2} is the upper critical field determined for YBCO single crystals.

linear up to a field H_{pG}. The slope between H^* and H_{pG} ($dM/dH\approx 0.045$ emu/Oe cm^3) is consistent with expectations for an 81%-dense sample in which the field has fully penetrated between the grains by H^* and the linear behavior observed results from the complete screening of individual grains. The temperature dependencies of H_{pJ}, H^*, and H_{pG} are plotted in Fig. 2

Further support for this interpretation is found in inset (b) of Fig. 3, which shows $M(H)$ measurements on the same poly-YBCO material after it was ground into a fine powder, then dispersed and set in epoxy. After grinding, the extremum at H_{pJ} is no longer evident. In addition, the other peaks (evident in Fig. 3), observed at H values of the sample magnitude as H_{pJ}, are also eliminated by powdering the sample. The shape of the $M(H)$ curves are also quite notable, in that the dependence of the hysteresis is far more characteristic of surface-barrier effects[14] than it is of bulk-pinning effects.[15] Except for the features near $H\approx|H_{pJ}|$, the shape of the $M(H)$ curve is retained after powdering, suggesting that this particular $M(H)$ dependence is related to the behavior of single grains. This particular behavior is that observed for very clean (low-defect density) single crystals.

Using flux trapping experiments it was possible to determine that the $M(H)$ behavior is completely reversible for applied fields up to about H_{pJ}, however, at fields above H_{pJ} a weak irreversibility begins to be observed.[10] At fields between H^* and H_{pG} the $M(H)$ curve is linear and fairly reversible. When H is reduced to zero from this field range, a remanent magnetization, about the same size as that observed for fields between H_{pJ} and H^*, is observed. Above H_{pG} there is a deviation from linearity and a much stronger irreversibility (larger remanent magnetization) is observed. These results suggest that complete screening of individual grains occurs between H^* and H_{pG} and then above H_{pG} fluxons begin to penetrate into the grains.

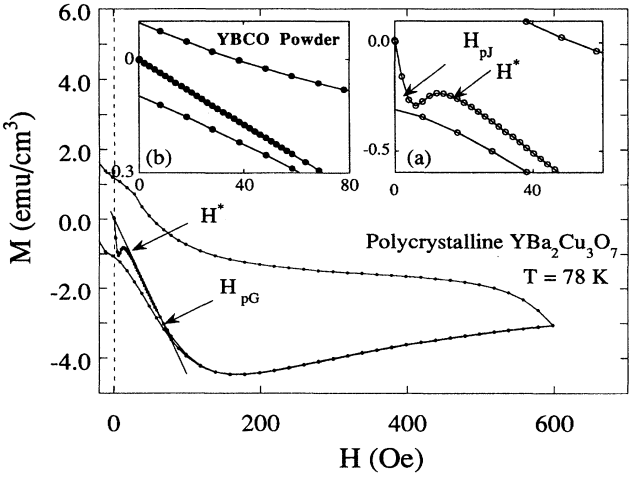

FIG. 3. Magnetization as a function of applied field $M(H)$ diagram. Inset (a) shows the initial portion of the $M(H)$ curve for an 81%-dense bulk polycrystalline YBCO sample while inset (b) shows the same region after powdering the sample.

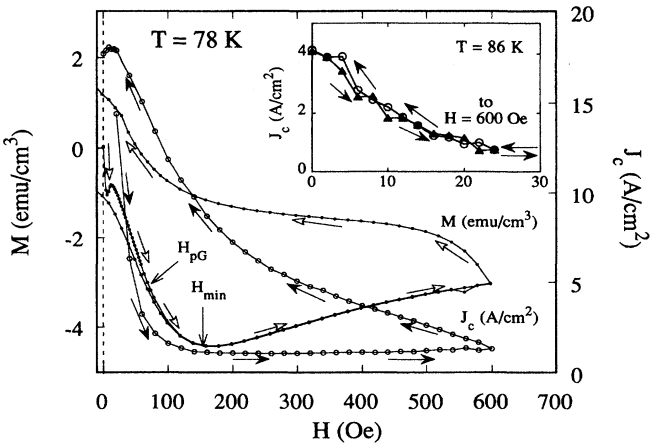

FIG. 4. A transport measurement of the critical current density J_c as a function of applied magnetic field $J_c(H)$ for temperatures below T_l. The inset shows J_c as a function of applied magnetic field $J_c(H)$ above T_l. For $H>22$ Oe the $E(J)$ curves used to define J_c no longer have negative curvature.

The $E(J)$ curves and their scaling, shown in Fig. 1, are remarkably similar to the curves observed for both disordered single crystals and epitaxial thin films of YBCO.[3,9] The scaling is strong support for the occurrence of a continuous phase transition at T_{cp} with the critical scaling coefficients $\nu \approx 1.0$ and $z \approx 4.0$. These values are consistent with a previous observation in poly-YBCO (Ref. 11) and with numerical simulations using a gauge glass model.[16] The value of the spatial critical exponent is lower than the value usually observed in YBCO thin films ($\nu = 1.7 \pm 0.2$).[3,5,17] This phase transition in poly-YBCO may physically be interpreted as being due to the distribution of supercurrent loops in the percolation network formed from the weakly-linked YBCO grains, which freeze-in randomly-oriented flux vortices at the transition.[18] The transition to this phase is theoretically predicted to occur when the Josephson coupling energy between the grains is on the order of kT.[19]

Evident in Fig. 2 is the overlap of $H_{cp}(T)$ with $H_{pG}(T)$ in the region where $H_{cp}(T)$ has the smaller slope. In addition, as seen more clearly in the inset of Fig. 2, $H_{pJ}(T)$ drops to zero at a point defined as T_l, which is in the region where $H_{pG}(T)$ changes slope. The slope of $H_{cp}(T)$ changes by a large amount in the region where $H_{pG}(T)$ comes to overlap $H_{cp}(T)$. This result is consistent with models of granular superconductivity, with the exception that $H_{pG}(T)$ replaces H_{c1} in these models.[19] This slope change is attributed to the fact that penetration of the flux into the grains reduces the flux compression between the grains, thereby reducing the flux density at the superconducting weak links between the grains.[20,21] The coincidence of the $H_{cp}(T)$ and $H_{pG}(T)$ boundaries at small H may be an artifact of the operational definition of $H_{pG}(T)$, since the changes that take place at $H_{cp}(T)$ transition may cause the $M(H)$ behavior to deviate from linearity at fields less than $H_{pG}(T)$.

Measurements of the critical current density J_c as a function of applied field are shown in Fig. 4 along with the associated $M(H)$ curve at that temperature. Several features are evident. First, at temperatures below T_l [or below where $H_{pG}(T)$ and $H_{cp}(T)$ overlap], $J_c(H)$ drops very rapidly as field increases up to H_{pG}. Near H_{pG} it is seen that the rate of decrease of $J_c(H)$ is significantly reduced and after reaching a field $H_{\min}$, which in this case is about two times the value of H_{pG}, $J_c(H)$ is no longer decreasing. In fact, above $H_{\min}$, $J_c(H)$ actually increases slowly with field. This is in strong contrast to the $J_c(H)$ behavior at temperatures above T_l, where the transition field H_{cp} is reached before flux can penetrate into the grains. As seen in the inset of Fig. 4, J_c drops rapidly and monotonically at temperatures above T_l. For $T>T_l$ and $H>22$ Oe at $T=86$ K, the $E(J)$ curves no longer exhibit negative curvature over the full current range measured.

It may be possible to explain the differences between J_c measured magnetically and J_c measured by transport using the results presented in Fig. 2.[22] In transport measurements, an arbitrary voltage criterion is usually used to define J_c, when in fact applying such a criterion to an $E(J)$ curve without negative curvature is meaningless; since positive curvature implies a linear resistance contribution. The presence of a linear resistance will rapidly dissipate a supercurrent generated magnetically in the same sample. Thus a J_c value determined using an arbitrary voltage criterion will continue to be observed well above H_{cp}, where the sample is actually no longer in a true superconducting state characterized by zero linear resistance.

In summary, using magnetic and magnetotransport measurements, a magnetic phase diagram for poly-YBCO was constructed. This magnetic phase diagram is fairly consistent with phase diagrams for granular superconductors.[11] It was shown that in magnetic fields up to H_{pJ}, the sample bulk (sample volume) was screened by supercurrents. As field increases above H_{pJ} flux begins to penetrate between the grains and near a field H^* the field has fully penetrated between grains. Between H^* and H_{pG} the volume of the individual grains is screened, while above H_{pG} the flux begins to penetrate into the grains. Between H^* and H_{pG}, when the flux is completely excluded from the grains, there is consid-

erable flux compression between the grains that results in a rapid drop in J_c with H. Once flux begins to penetrate into the grains, the rate of J_c decrease is lowered, and where the flux penetration rate meets or exceeds the increase in applied field ($\approx H_{\min}$), J_c actually starts to increase with H. In addition, based on scaling of $E(J)$ results, there is strong evidence of a true thermodynamic-phase transition to a state characterized by zero linear resistance. This transition does not appear to be determined by intragranular vortex motion, but rather to be characterized by intergranular properties. The $M(H)$ dependence observed in poly-YBCO is much more consistent with flux penetration into grains that is limited by surface barriers than by bulk pinning. This suggests that the individual grains of poly-YBCO are weakly disordered. In contrast to this, ZFC/FCC magnetic results are more characteristic of a strongly-disordered system, however, the interpretation of this boundary is as yet unclear for poly-YBCO. The ZFC/FCC boundary can probably be best described as the upper bound for irreversible behavior whether that behavior is intra- or intergranular in nature.

We would like to thank S. Gerber, G. Giuliani, M. Konczykowski, H. Nakanishi, M. E. McHenry, and T. M. Shaw for valuable discussions and M. Darwin for technical assistance. This work was supported by the Director for Energy Research, Office of Basic Energy Sciences through the Midwest Superconductivity Consortium (MISCON) DOE Grant No. DE-FG02-90ER45427.

[1] M. P. A. Fisher, Phys. Rev. Lett. **62**, 1415 (1989); D. S. Fisher, M. P. A. Fisher, and D. A. Huse, Phys. Rev. B **43**, 130 (1991).

[2] M. V. Feigel'man, V. B. Geshkenbein, and A. I. Larkin, Physica C **167**, 177 (1990); M. V. Feigel'man, V. B. Geshkenbein, and V. M. Vinokur, Phys. Rev. B **43**, 6263 (1991).

[3] R. H. Koch, V. Foglietti, W. J. Gallagher, G. Koren, A. Gupta, and M. P. A. Fisher, Phys. Rev. Lett. **63**, 1511 (1989).

[4] P. L. Gammel, L. F. Schneemeyer, and D. J. Bishop, Phys. Rev. Lett. **66**, 953 (1991).

[5] J. Deak, M. McElfresh, R. Muenchausen, S. Foltyn, and R. Dye, Phys. Rev. B **48**, 1337 (1993).

[6] T. Schuster, M. R. Koblischaka, B. Ludescher, R. Henes, A. Kottmann, and H. Kvonmuller, Mater. Lett. **14**, 189 (1992).

[7] J. P. Singh, R. A. Guttshow, J. T. Dusek, and R. B. Poeppel, J. Mater. Res. **7**, 2324 (1992).

[8] K. A. Müller, M. Tagashige, and J. G. Bednorz, Phys. Rev. Lett. **58**, 1143 (1987).

[9] J. Deak, M. McElfresh, John R. Clem, Zhidong Hao, M. Konczykowski, R. Muenchausen, S. Foltyn, and R. Dye, Phys. Rev. B **47**, 8377 (1993); J. Deak, M. McElfresh, John R. Clem, Zhidong Hao, M. Konczykowski, R. Muenchausen, S. Foltyn, and R. Dye, *ibid.* **49**, 6270 (1994).

[10] M. W. McElfresh, Y. Yeshurun, A. P. Malozemoff, and F. Holtzberg, Physica A **164**, 308 (1990).

[11] T. K. Worthington, E. Olsson, C. S. Nichols, T. M. Shaw, and D. R. Clarke, Phys. Rev. B **43**, 10 538 (1991).

[12] H. Safar, P. L. Gammel, D. A. Huse, D. J. Bishop, J. P. Rice, and D. M. Ginzburg, Phys. Rev. Lett. **69**, 824 (1992).

[13] Z. Hao, J. R. Clem, M. W. McElfresh, L. Civale, A. P. Malozemoff, and F. Holtzberg, Phys. Rev. B **43**, 2844 (1991).

[14] C. P. Bean and J. D. Livingston, Phys. Rev. Lett. **12**, 14 (1964); M. Konczykowski, L. Burlachkov, Y. Yeshurun, and F. Holtzberg, Phys. Rev. B **43**, 13 707 (1991).

[15] C. P. Bean, Rev. Mod. Phys. **36**, 31 (1964).

[16] J. D. Reger, T. A. Tokuyasu, A. P. Young, and M. P. A. Fisher, Phys. Rev. B **44**, 7147 (1991).

[17] C. Dekker *et al.*, Phys. Rev. Lett. **68**, 3347 (1992); Y. Ando *et al.*, *ibid.* **69**, 2851 (1992); D. G. Xenikos *et al.*, Phys. Rev. B **48**, 7742 (1993); H. K. Olsson *et al.*, *ibid.* **66**, 2661 (1991); Hiu Wu *et al.*, Phys. Rev. Lett. **71**, 2642 (1993).

[18] S. John and T. C. Lubensky, Phys. Rev. B **34**, 4815 (1993).

[19] A. Gerber, T. Grenet, M. Cyrot, and J. Beille, Phys. Rev. B **45**, 5099 (1992).

[20] J. E. Evetts and B. A. Glowacki, Cryogenics **28**, 641 (1988).

[21] Shi Li, M. J. Darwin, J. Deak, D. Majer, P. Metcalf, E. Zeldov, and M. McElfresh, Physica C **236-240**, 3091 (1994).

[22] A. P. Malozemoff (private communication).